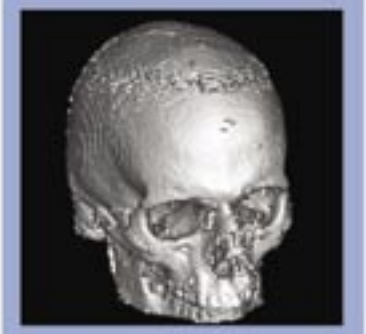

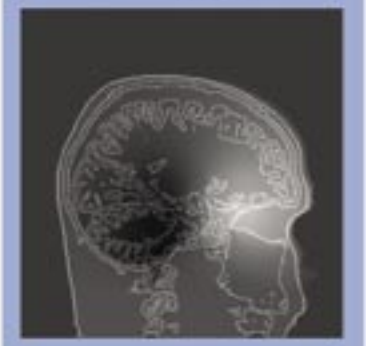

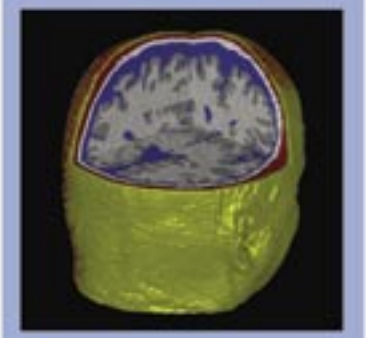

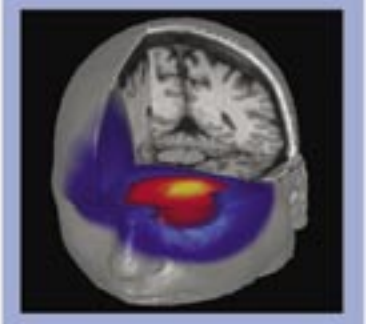

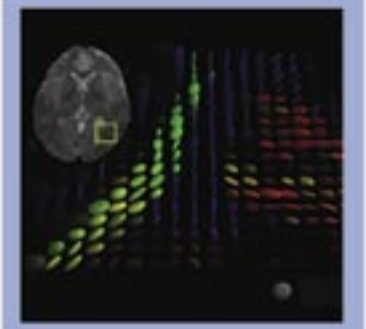

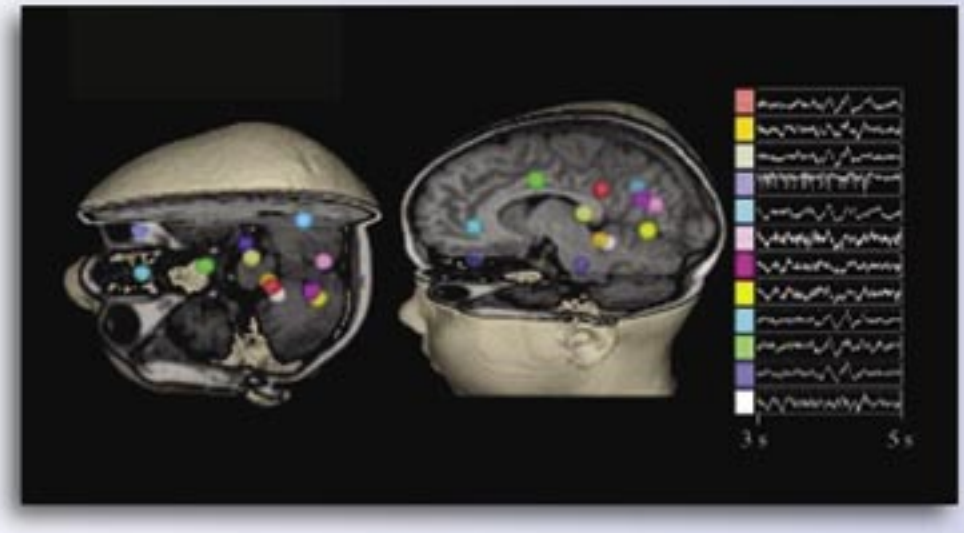
3 s
5 s

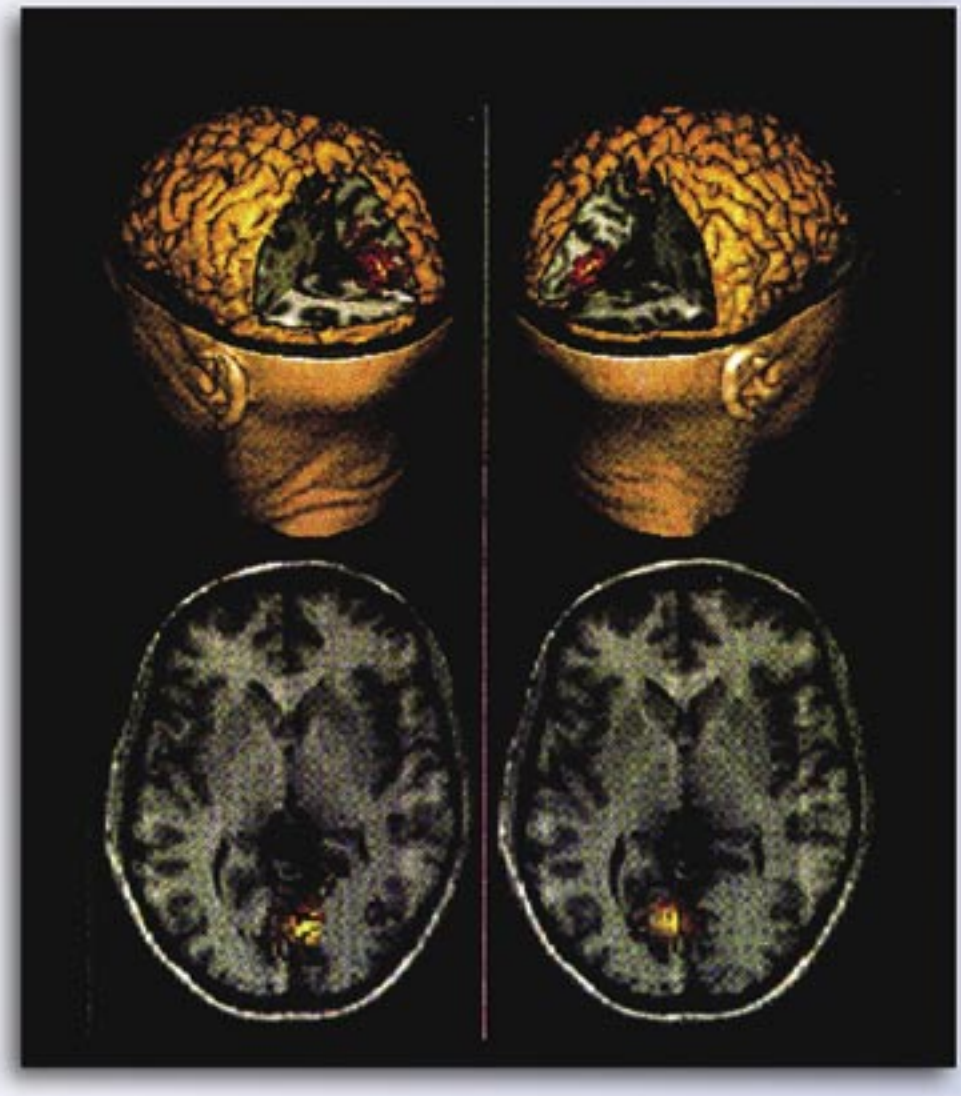

Biophysics

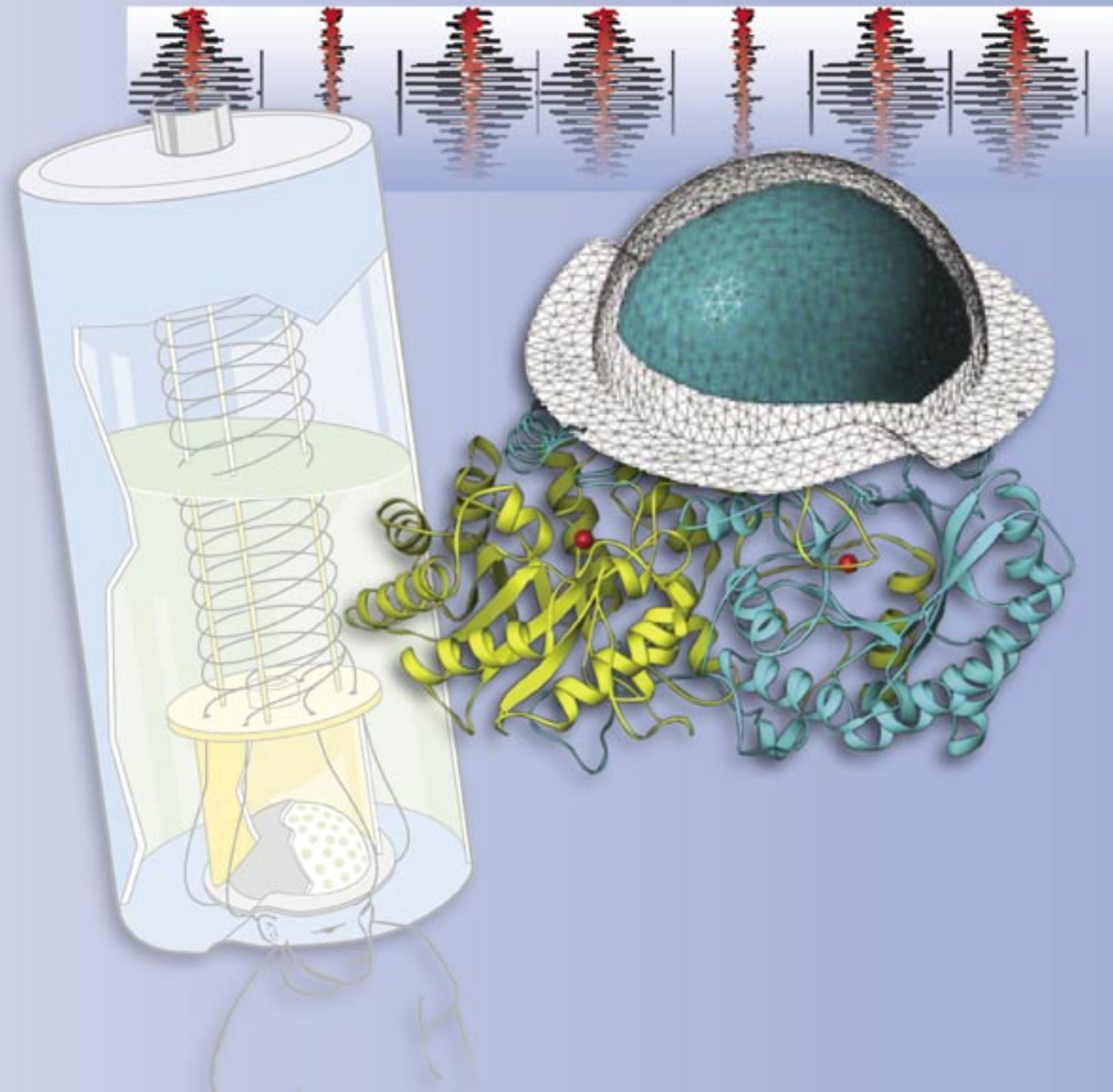

Biophysics Contents

Research Highlights

Project Descriptions

Multi-Modality Imaging and Modeling of Dynamic Brain Function

J.S. George, D.M. Schmidt, C.C. Wood, G. Kenyon (P-21), B.J. Travis (EES-2)

The past few decades have witnessed extraordinary progress in the development of techniques for structural and functional imaging of the human brain. MRI is the premier technique for imaging the soft tissue anatomy of the human brain, but it has significant limitations for defining the geometry of the skull, which computerized tomography does very well. Functional MRI provides detailed pictures of spatial patterns of neural activation based on associated hemodynamic changes but does not capture the characteristic temporal dynamics of neurophysiological activation. MEG and EEG provide excellent temporal resolution of neural population dynamics but are limited in spatial resolution by the ambiguity and ill-posed nature of the source reconstruction problem. Electrophysiology, microanatomy, optical imaging, and other methods each provide important though limited insight into neural function and functional organization. Although the mix and relative importance of imaging technologies will evolve, the need to integrate information from multiple methods will remain.

Dynamic neuroimaging techniques allow measurement of neural population responses that reflect integrated activity of the underlying networks. Evolving analytical strategies allow increasingly reliable source localization and time-course estimation based on MEG and EEG, incorporating anatomy from MRI.[1,2] These tools allow us to observe the dynamic responses of neural populations; but to understand the nature and basis of network function, it is necessary to build models. Computational models of the physical systems and of the physiological processes that give rise to observable responses are essential to connect experimental measures with models of the distribution and dynamics of neural activation. *Forward models* of field or potential distributions at the head surface associated with primary currents within the brain are the basis for *inverse procedures* for MEG and EEG that attempt to estimate the

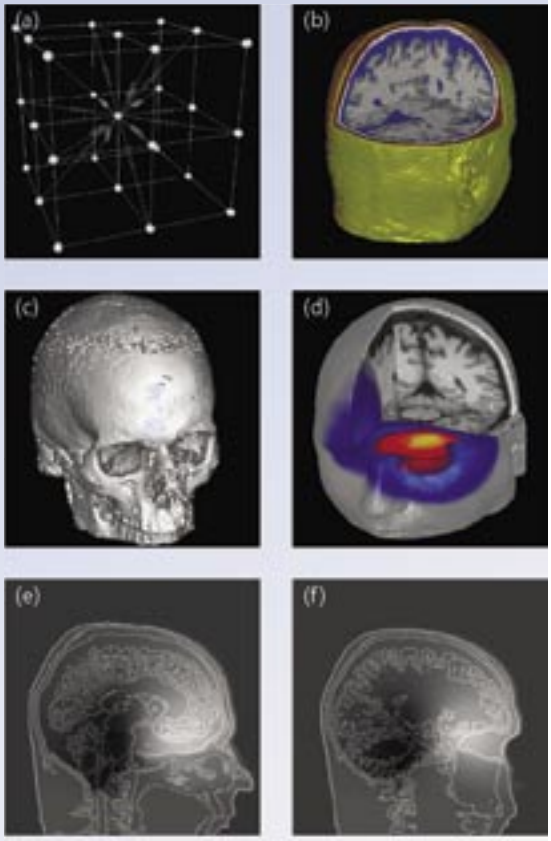

Figure 1. Forward calculations by the FDM. (a) Influence scheme showing resistive links between neighboring nodes. (b) Segmented MRI used to set conductivities for simulation. (c) Skull segmented from MRI before post processing. (d) Surface/cut plane rendering of potentials from Figure 1(c). (e and f) Two slices through computed potential volume, showing current leakage along the optic nerve penetration. (g) Computed conductivity tensors based on DT-MRI. Note the anisotropy of conductivity corresponding to white matter tracts.

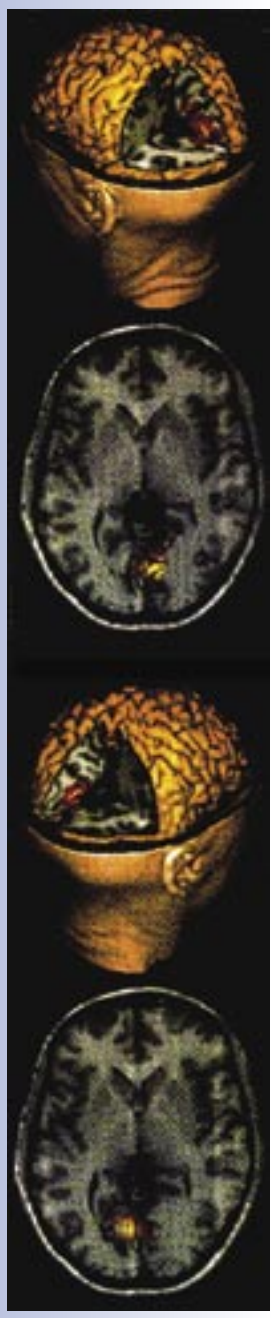

Figure 2. Bayesian Inference probability maps of source locations derived from MEG studies of visual responses.

number, location, extent, and time courses of regions of cortical activation. Simulation tools that capture the three-dimensional architecture and functional dynamics of neurons and of extended networks allow us to predict interesting dynamic responses and to optimize network models that account for experimental observations.

Advanced Forward Models

Source localization based on MEG and EEG has traditionally employed analytical or semi-analytical forward calculations based on simple geometries such as spherical shells, assuming that errors introduced by the forward calculation are small relative to the uncertainty associated with the inverse estimation procedure. For some applications, boundary element methods have been used, incorporating the gross geometry of the major conductivity boundaries of the head and employing a small number of tissue classes of simplified geometry.[1] However, as inverse methods get better, the simplifying assumptions inherent in these methods are less tenable.

Finite difference calculation. We have adopted an alternative strategy based on a finite difference method (FDM) that can incorporate more detailed geometry based on MRI and estimates of volume conductivity provided by emerging imaging methods, including diffusion tensor (DT) MRI, current density MRI, and electrical impedance tomography. FDM does not require construction of a specialized computational mesh or explicit identification and topological checking of boundaries; the calculation is performed on a rectangular grid that is the most natural representation of the MRI data used to define the geometry. Various techniques improve the performance of the FDM on a rectangular grid, e.g., adaptive mesh refinement to control error in regions with high field variation and formulations that reduce errors caused by the staircase approximation of a curved boundary.

Because the FDM allows easy manipulation of geometrical details of the volume conductor, we have examined the effects of skull penetrations on observed field distributions. These studies demonstrated significant effects of the optic nerve and ear canal on both the magnitude and distribution of the potential field compared to a model that did not incorporate these shunts (Figure 1). These effects might significantly influence localization of sources in frontal or temporal lobes. We anticipate that it will be important to account for surgical penetrations of the cranium for neurosurgical patients in whom source localization studies are undertaken.

Conductivity estimation. Although our computational formalism handles anisotropic conductivity, in the past such capability was of little consequence because there were no methods for the noninvasive estimation of tissue conductivity or anisotropy. However, our recent work has demonstrated the feasibility of estimating anisotropic conductivity based on DT-MRI [Figure 1(g)]. Tuch[3] has shown that DT-MRI has a well-defined relationship to tissue conductivity. Diffusion and conductivity tensors share the same eigenvectors as a result of the common microgeometry. The relationship between the eigenvalues for diffusion and conductivity can be derived using an "effective medium" theory; we conclude that conductivity and diffusion are strongly and linearly related. Advances in measurement technology and analytical procedures may allow estimation of head conductivity using electrical impedance tomography coupled with models of tissue geometry from MRI.

The Neural Electromagnetic Inverse Problem

To estimate the dynamics of neural systems, an adequate model of the spatial distribution of the underlying sources is needed. Building this source model is the principal business of inverse procedures. Over the past decade, we and others have made significant advances in the development and implementation of inverse procedures for MEG and EEG. Increasingly, these methods employ information derived from other imaging modalities such as MRI to inform or constrain source localization procedures.

Bayesian Inference. We have previously described a technique for Bayesian Inference that addresses the fundamental ambiguity of the inverse problem and the complex error surface associated with the model parameter space by explicitly sampling the posterior probability distribution.[4] A Markov Chain Monte Carlo (MCMC) technique is used to conduct a series of numerical experiments and to see which stochastic solutions best account for the data (Figure 2). Source models accommodate an extended region of activation within a bounding volume defined by a few parameters. Because Bayesian methods explicitly employ prior

knowledge to help solve the inverse problem, they provide a natural and formal method to integrate multiple forms of image data.

Parametric distributed source model. In the 1999 paper describing Bayesian Inference,[4] we employed a parametric source model consisting of a set of elemental currents, each aligned orthogonal to the local cortical surface and all contained with a bounding sphere centered on some cortical voxel. We recently have implemented a new technique to define the bounding volume for our activation model that produces regular two-dimensional patches across the cortex sheet. The patch is defined by a series of dilation operations (i.e., stepwise labeling of successive layers of contiguous voxels) about some seed voxel. This method produces source models based on patches of cortical activation, more consistent with our expectations, and allows useful constraints on the polarity of cortical currents.

Spatio-Temporal Bayesian Inference. Our initial formulation of Bayesian Inference was applied to single instantaneous field maps. However, our experience has underscored the value of spatio-temporal modeling procedures that attempt to fit an extended sequence of field maps across time with a consistent ensemble of sources. This strategy produces a more parsimonious model and exploits the strong, local correlation within the time domain of integrated neural population activity. We have developed a scheme for Spatio-Temporal Bayesian Inference (STBI) in which each parametric model source has an associated time course. The MCMC algorithm is used to sample the posterior probability distribution of the time courses structured as vectors with an element corresponding to each time point of the sampled field distributions. By this strategy, we are able to estimate the form and variance of the time course associated with each probabilistic source.

Studies with simulated data. Figure 3 outlines the results of a numerical study applying STBI to a simulated data set. In this example, we defined three small, distributed sources. Two of the sources have time courses that are highly correlated—a condition that creates difficulties for some spatio-temporal methods. STBI recovered all three of the sources and time courses with surprising fidelity and with very tight confidence intervals. In another study, we were able to resolve two sources separated by less than a centimeter near the posterior pole of occipital cortex on the basis of differences in orientation and time course. Our experience with simulated data suggests that much of the ambiguity of the MEG inverse problem is eliminated by STBI.

Coupling Experiments and Network Models

In spite of the advances in analytical methodology, noninvasive methods are unlikely to ever provide the spatial and temporal resolution required to monitor the activity of the entire ensemble of individual neurons in a local circuit within the brain. Network-modeling techniques offer the only viable strategy to truly understand dynamic measures of brain function in terms of the underlying synaptic and cellular dynamics and network connectivity. To do this properly, we must model at least some of the physiological and geometrical complexity of real neurons while accommodating very-large-scale networks.

Visual system model. The mammalian visual system represents an ideal structure for employing cellular-level network models to relate dynamic measures of neural activity to underlying neural architecture and population dynamics. In the retina, cellular-network simulations can be related to measures of activity provided by individual microelectrodes or electrode arrays or by dynamic-optical-imaging techniques, thus providing a method to validate and optimize the first steps of the system simulation. We have already used such models to predict and account for experimentally observed dynamic responses.[5]

Large-scale, biologically realistic networks are modeled with the Sensory Enhanced Neural Simulation Engine (SENSE)—a general-purpose neural simulator originally developed by LANL investigators.[6] SENSE can model systems containing as few as one neuron up to millions of geometrically and physiologically realistic neurons. SENSE has recently been implemented as a parallel code to increase the size and complexity of tractable models. With high-performance computers, extended systems such as the early visual pathways can be simulated. SENSE has been coupled to conjugate

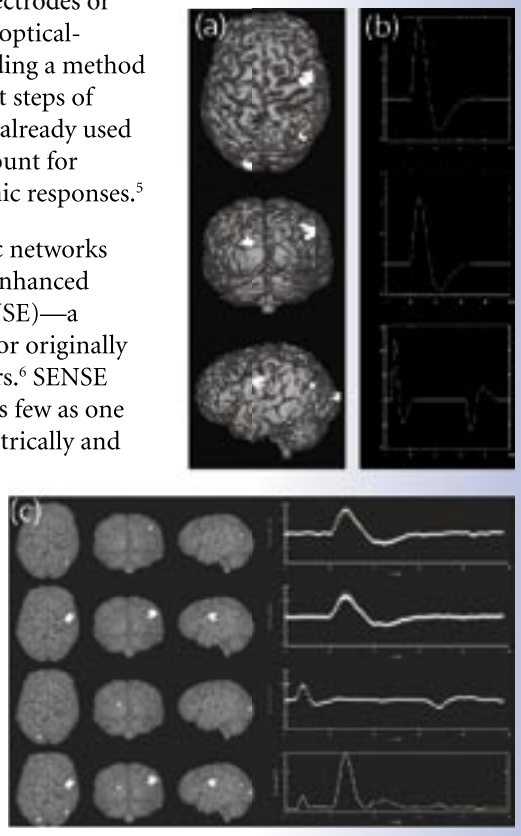

Figure 3. Source location and dynamics estimated by STBI. (a) Locations and (b) timecourses of simulated sources. (c) Locations and timecourses estimated by STBI.

gradient-based inverse and optimization algorithms, allowing data fitting or optimization as a function of any SENSE variable or combination of variables.

Extensions for physical modeling. SENSE captures the realistic three-dimensional spatial arrangements and connectivity patterns of neurons seen in neural tissue and the geometric, electrochemical, and synaptic properties of individual neuronal types. Evolution of the voltage of each neuron's compartments is computed through a series of time steps. We have exploited this capability to compute the net current vector associated with activation of an individual neuron or population of neurons. Such a model can be coupled with the forward models previously described to predict patterns of response observable with MEG or EEG.

Optimization and applications of network models. We have begun to compare model network responses to functional imaging data at the cellular-network level in order to disclose dynamic spatial and temporal patterns of activation that underlie interesting functional properties of neuronal networks. We continue to develop a network model of the retina that can be fit to experimental ensemble data produced with electrode arrays and optical imaging techniques in an effort to optimize neuronal and network properties. We have prototype models of much of the early visual system, and we will calibrate coupled-system model parameters against MEG and EEG data using efficient optimization algorithms to produce quantitative models of neural electromagnetic responses. This work is motivated by our role in a DOE-sponsored project to develop an electroneural prosthetic retinal implant.

Conclusion

Computational integration of multiple techniques for structural and functional neuroimaging provides a much more powerful strategy for dynamic measurement of brain function than the use of any individual method in isolation. Network models allow us to generate experimentally testable predictions of network behavior, such as modulation of dynamic activity and phase-locked oscillations within a population that should set up large signals detectable by MEG or EEG. Such responses are of increasing theoretical interest for understanding the computation by the brain.

References

1. J.S. George, C.J. Aine, J.C. Mosher, D.M. Ranken, H.A. Schlitt, C.C. Wood, J.D. Lewine, J.A. Sanders, and J.W. Belliveau, "Mapping function in the human brain with MEG, anatomical MRI, and functional MRI," *Journal of Clinical Neurophysiology* **12**(5), 406-431 (1995).
2. J.S. George, D.M. Schmidt, D.M. Rector, and C.C. Wood, "Dynamic functional neuroimaging integrating multiple modalities," in *Functional MRI: An Introduction to Methods* (Oxford University Press, United Kingdom, 2001)**,** pp. 353-382**.**
3. D.S. Tuch, V.J. Wedeen, A.M. Dale, J.S. George, and J.W. Belliveau, "Conductivity tensor mapping of the human brain using diffusion MRI," in *Proceedings of the National Academy of Science* **98**,11697-11701 (2001).
4. D.M. Schmidt, J.S. George, and C.C. Wood, "Bayesian Inference applied to the electromagnetic inverse problem," *Human Brain Mapping* **7**, 195-212 (1999).
5. G.T. Kenyon, B. Moore, J. Jeffs, G.S. Stephens, B.J. Travis, J.S. George, J. Theiler, and D.W. Marshak, "A model of high frequency oscillatory potentials in retinal ganglion cells," *Visual Neuroscience* (in press).
6. S. Coghlan, M.V. Gremillion, and B.J. Travis, "NeuroBuilder: A user interface and network simulator for building neurobiological networks," in *Analysis and Modeling of Neural Systems I*, F.H. Eeckman, Ed. (Kluwer Academic Publishers, Massachusetts, 1992), pp. 115-122.

Acknowledgment

This work was supported, in part, by the LANL LDRD program, the MIND Institute, and NIH.

For more information, contact John George at 505-665-2550, jsg@lanl.gov.

Computer Models of Neural Circuits

G.T. Kenyon, G.J. Stephens, M.C. Flynn, J.S. George, J.M Galbraith (P-21), B.J. Travis (EES-2), J. Theiler (ISR-2)

We are using computer simulations to study the dynamics of neural circuits. Although much is known about the inner workings of individual nerve cells, called neurons, the operational principles governing the dynamics of complex interconnected networks of neurons remain poorly understood. By simulating large, heterogeneous neural systems on modern digital computers, we hope to discover some of the operational principles that underlie the extraordinary processing power of biological computers. A better understanding of biological computation will likely contribute to the development of new technologies for treating neurological disease and may well lead to revolutionary advances in machine intelligence.

Understanding Information Processing in the Vertebrate Retina

Many of our studies to date have been directed toward understanding information processing in the vertebrate retina. The retina has many advantages as a target system for developing realistic computer models. The anatomy and physiology of the retina have been extensively studied, especially in comparison with many other parts of the central nervous system; the inputs and outputs of the retina can be well characterized; and the retina receives no major feedback projections from the brain, allowing it to be treated as a stand-alone circuit. Furthermore, we may reasonably expect that by understanding how the retina talks to the brain, we will gain fundamental insight into how the different parts of the brain talk to each other. The following results were obtained using a computer model of the cat retina that has allowed us to investigate the function of retinal circuitry at a level that would be very difficult with currently available experimental techniques.[1]

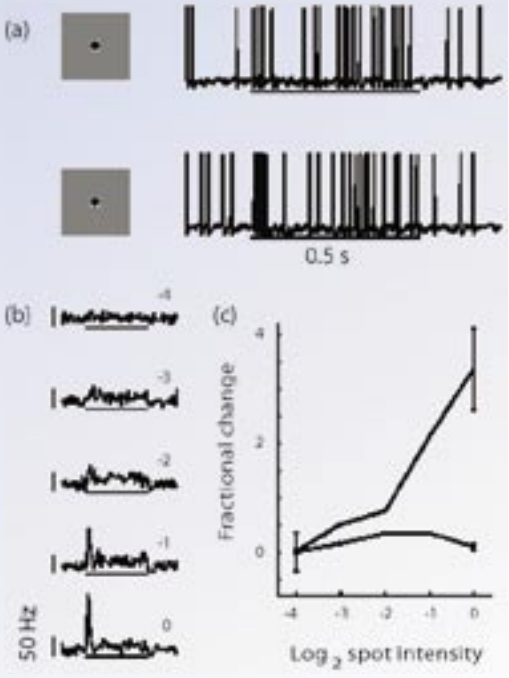

Figure 1. Responses of model ganglion cells to small spots. (a) Ganglion-cell output consists of discrete, uniform pulses. A relatively dim spot (top) produces a small increase in the firing rate, whereas a relatively bright spot (bottom) produces a large transient peak in the firing rate. (b) Peri-stimulus time histograms, giving the change in firing rate versus time, are plotted for various spot intensities (log_2 units). (c) Plot of peak (solid line) and plateau (long-short dashed line) firing rate as a function of spot intensity. Local inhibition prevents the plateau-firing rate from increasing significantly with stimulus intensity.

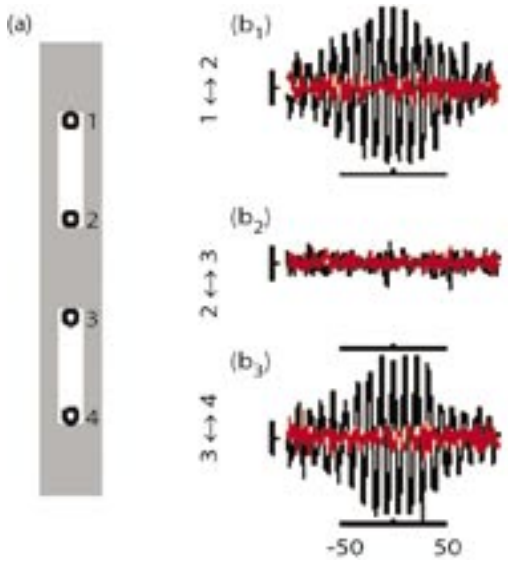

Figure 2. Stimulus-selective synchronization of ganglion cells. (a) Stimulus dimensions relative to the receptive field centers of individual ganglion cells. (b) Cross-correlation histograms computed during the plateau portion of the response between spike trains from pairs of ganglion cells at opposite ends of the same bar or at opposing tips of separate bars. All ganglion-cell pairs were separated by 7 diameters (bin size: 1 ms; scale: 100 ms, 0.5). Also, b_1 is the pair from the upper bar; b_2 is the pair from separate bars; and b_3 is the pair from the lower bar. Correlations were only significant for pairs from the same bar.

Our most intriguing finding is that retinal neurons can encode visual information in rather surprising ways. The output of a neuron cannot be classified in conventional electrical engineering terms as either analog or digital, but rather it consists of something altogether different—a temporal sequence of impulses, or spikes. Because each spike is (to a first approximation) identical to every other spike, information can only be conveyed by the temporal pattern of impulses. Neuroscientists continue to debate how information is encoded within the temporal structure of neural spike trains, but there is widespread agreement that one very important variable is the firing rate. Figure 1 shows an example of how a typical neuron in our retinal model encodes the local intensity, or contrast, of a small stimulus as a transient increase in firing rate.

About 10 years ago, Wolf Singer's laboratory in Germany reported that retinal neurons use the relative timing of spikes to encode global information about visual stimuli that is not conveyed by their local firing rates.[2,3,4] Using our retinal model, we were able to demonstrate a very similar phenomenon by examining the relative timing of spikes produced by neurons responding to either the same or to different objects (Figure 2). For retinal neurons activated by the same large object, their spike trains were strongly correlated, or phase locked, by a common underlying oscillation at a frequency of approximately 100 Hz. Pairs of retinal neurons activated by different objects, however, were not correlated because the phases of their underlying oscillations varied randomly with respect to each other. Thus, our retinal model captures the interesting property of biological neurons—their evoked oscillations in responses to appropriate large visual features are stimulus-specific and are only phase-locked between cells responding to the same contiguous object.

We used the retinal model to ask what information-stimulus-specific oscillations between retinal neurons might convey to the brain. To investigate this question, we were guided by two principles. (1) Because it only takes us a fraction of a second to form a visual impression, the information conveyed by stimulus-specific oscillations must be available on short, physiologically meaningful time scales—roughly a few hundred milliseconds. (2) Because the spatial convergence of retinal neurons onto target cells in the brain is rather low, with each target cell receiving input from only a few retinal neurons, the information conveyed by stimulus-specific oscillations must be available locally in the firing activity of a similarly small number of neighboring cells. We thus used the retinal model to quantify the information conveyed about the global properties of a stimulus—in this case, the total size of the object—by a 2 × 2 neighborhood of retinal output neurons in a few hundred milliseconds. At the same time, we were fortunate to receive data from Wolf Singer's laboratory recorded from output neurons in the cat retina under similar experimental circumstances. These data allowed us to directly test the predictions of our retinal model.

The oscillations evoked by stimuli of various sizes in our retinal model were very similar to those measured from the cat retina (Figure 3). In both sets of data, small stimuli evoked little or no oscillatory response, whereas large stimuli evoked very large oscillations. Because our model is consistent with the known anatomy and physiology of the cat retina, it can provide a useful tool for investigating how information may be encoded by spike trains in the optic nerve.

Why Stimulus Size Matters

To determine the information content of both artificial and biological spike trains, we asked whether it was possible to determine if a group of neighboring cells was responding to a small or large object using their local firing activity alone (Figure 4). Our results are plotted as a percent correct, which was proportional to the fraction of trials on which the total size of the stimulus could be correctly inferred from the local firing activity. Random events were added to the model spike trains to ensure that the average number of spikes, or firing rate, did not change as a function of stimulus size. The only cue available from the local firing activity regarding the total size of the stimulus was therefore the amplitude of the synchronous oscillations. Our results showed that in 300 ms (using as few as 4 spike trains from a small 2 x 2 neighborhood), it was possible to achieve performance levels approaching 90% correct.

In related experiments, we showed that there was a tradeoff between the number of cells included in the analysis and the total time allowed for accomplishing the size discrimination task. Specifically, as more cells were included in the analysis, shorter time windows were required to achieve the same performance levels.

Why, one might ask, is it important for retinal neurons to convey information about stimulus size in their local firing activity? For a possible answer to this question, consider the frog retina, where Tachibanna's laboratory in Japan has shown that there are specialized neurons, called dimming detectors, that exhibit strong synchronous oscillations when activated by a large dimming object but not when activated by a small dimming object.[5] Considering that from a frog's perspective, a small dimming spot might be a fly or other food source, whereas a large dimming spot is more likely to be a bird or other dangerous predator, one can quickly appreciate why size matters.

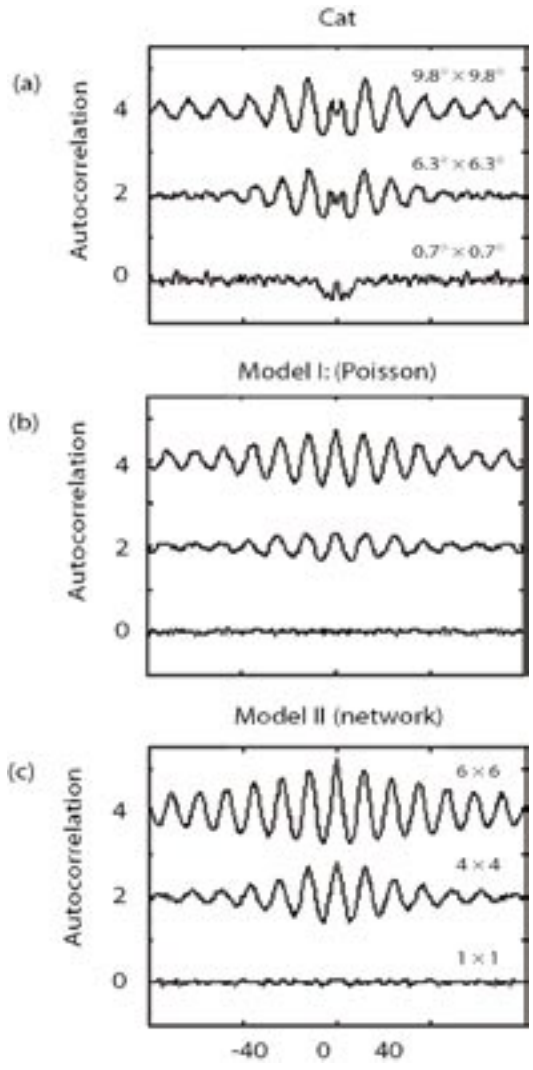

Figure 3. Multi-unit auto-correlograms and cross-correlograms reveal size-dependent high-frequency oscillations. (a) Auto-correlograms computed from multi-unit spike trains recorded from cat retina at the center-of-square spots of increasing size (data were re-plotted from Reference 3). Correlations are expressed as a fraction of the expected level due to chance. (b) Multi-unit cross-correlograms of artificial spike trains, generated by a Poisson process, containing four identically modulated units, each with a mean firing rate of 50 Hz. (c) Multi-unit cross-correlograms produced by an integrate-and-fire feedback circuit consistent with retinal anatomy. Multi-unit spike trains were recorded from a fixed 2 x 2 array of ganglion cells located at the center of each spot (intensity = -2). Poisson-distributed spikes were added to each train to maintain a constant mean firing rate of 50 Hz regardless of spot size.

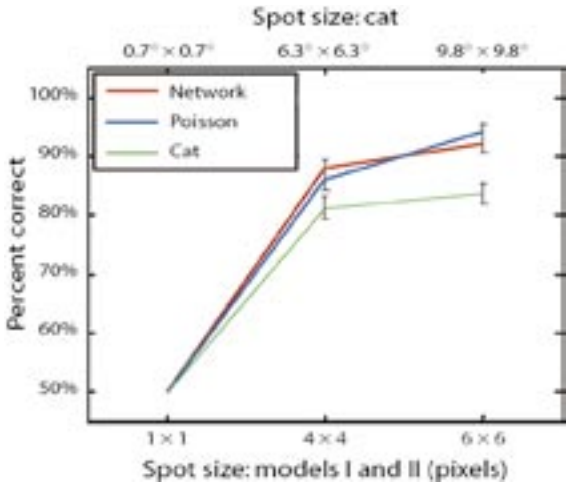

Figure 4. Theoretically optimal performance on a size-discrimination task. Individual 200-ms segments of multi-unit spike-train data were obtained in response to spots of one of two sizes: (1) either an intermediate or small spot (top abscissa = 6.3° x 6.3°, bottom abscissa = 4 x 4) or (2) either a large or small spot (top abscissa = 9.8° x 9.8°, bottom abscissa = 6 x 6). The ordinate gives the maximum percentage of trials that could be classified correctly, assuming each binary possibility was equally likely a priori, based on the total energy in the single-trial power spectra between 75 and 95 Hz. All three data sets indicate that high-frequency oscillations within a small group of ganglion cells yield good single trial discrimination of stimulus size.

References

1. G.T. Kenyon, B. Moore, J. Jeffs, K.S. Denning, G.S. Stephens, B.J. Travis, J.S. George, J. Theiler, and D.W. Marshak, "A model of high frequency oscillatory potentials in retinal ganglion cells," *Visual Neuroscience* (in press, 2003).
2. C.M. Gray, P. Konig, A.K. Engel, and W. Singer, "Oscillatory responses in cat visual cortex exhibit inter-columnar synchronization which reflects global stimulus properties," *Nature* **338**(6213), 334-337 (1989).
3. S. Neuenschwander, M. Castelo-Branco, and W. Singer, "Synchronous oscillations in the cat retina," *Vision Research* **39**(15), 2485-2497 (1999).
4. S. Neuenschwander and W. Singer, "Long-range synchronization of oscillatory light responses in the cat retina and lateral geniculate nucleus," *Nature* **379**(6567), 728-32 (1996).
5. H. Ishikane, A. Kawana, and M. Tachibana, "Short- and long-range synchronous activities in dimming detectors of the frog retina," *Visual Neuroscience* **16**(6), 1001-1014 (1999).

Acknowledgment

This work is supported by the LDRD program at LANL, by the Deployable Adaptive Processing Systems program funded by the DOE Office of Nuclear Nonproliferation, and by the DOE Office of Biomedical and Environmental Research.

For more information, contact Garrett Kenyon at 505-667-1900, gkenyon@lanl.gov.

SQUID Magnetometry—Harnessing the Power of Tiny Magnetic Fields

R.H. Kraus, Jr., M.A. Espy, A.N. Matlachov, P.L. Volegov, J.C. Kumaradas, C. Carr, V. Armijo, S.G. Newman, J. Mattson (P-21), W.P. Roybal (ESA-WMM)

Measurements associated with the neural currents in the brain can be used to diagnose epilepsy, stroke, and mental illness and to study brain function. One way to observe these tiny electrical currents is to measure the magnetic fields they produce outside the skull—a technique called magnetoencephalography (MEG).

The traditional way to monitor the brain's electrical activity is with EEG, which requires gluing as many as 150 electrodes to the scalp. MEG is a noninvasive technique that measures the direct consequence of neuronal activity in the living brain. MEG, together with EEG, are the only noninvasive techniques of measuring brain function at millisecond time resolution or better. MEG measures brain currents as precisely as EEG does but without physical contact, making it possible to screen large numbers of patients quickly and easily. MEG is also insensitive to the conductivities of the scalp, skull, and brain—which can affect EEG measurements.

Enter the SQUID

Measuring the brain's magnetic fields is not easy, however, because they are so weak. Just above the skull, they have strengths of 0.1 to 1 pT, less than a hundred millionth of the earth's magnetic field. In fact, brain fields can be measured only with the most sensitive magnetic-field sensor known—the superconducting quantum interference device (SQUID).

A SQUID is a loop of superconducting material interrupted by one rf or two dc resistive regions known as Josephson junctions. When cooled to very low temperatures, superconductors conduct electricity without resistance. This lack of resistance allows a SQUID to measure the interference of quantum-mechanical electron waves as the magnetic flux enclosed by the loop changes. A SQUID can measure magnetic fields as small as 1 fT.

Cohen first reported detecting a magnetic signal originating from the human brain in 1968 using a nonsuperconducting sensor.[1] Shortly thereafter, an rf SQUID sensor was used for the first time to measure a biomagnetic signal originating from the human heart,[2] and after only two more years, the same instrument was successfully used to record a human magnetic alpha rhythm with a satisfactory signal-to-noise ratio.[3] The first evoked-response magnetic signals associated with brain activity evoked by peripheral sensory stimulation measured with a SQUID sensor was reported in 1975.[4]

The LANL Superconducting Image Surface Whole-Head MEG System

The LANL SQUID team has designed and built a whole-head MEG system that uses 155 dc SQUIDs to provide simultaneous recordings of MEG activity over the entire head. The SQUIDs become superconducting when immersed in

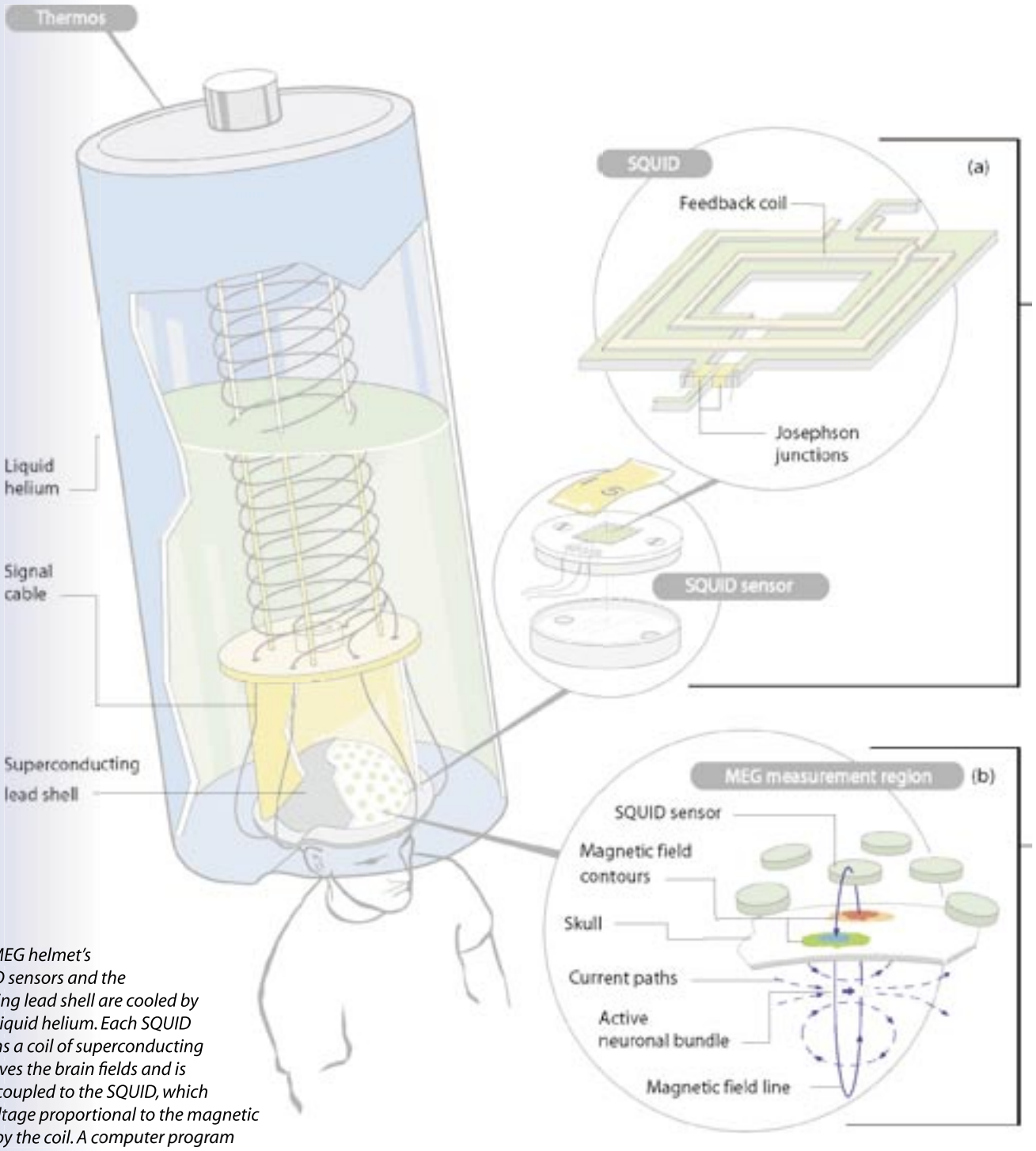

Figure 1. The MEG helmet's array of SQUID sensors and the superconducting lead shell are cooled by immersion in liquid helium. Each SQUID sensor contains a coil of superconducting wire that receives the brain fields and is magnetically coupled to the SQUID, which produces a voltage proportional to the magnetic field received by the coil. A computer program converts the SQUID data into maps of the currents flowing throughout the brain as a function of time. (a) The magnetic field lines that pass through the square hole at the SQUID's center determine the phases of electron waves circulating in the SQUID's superconducting region (green): the waves' interference is proportional to the magnetic flux over the hole. Because superconductors have no electrical resistance, the interference can be measured only by interrupting the superconductor with small regions that have electrical resistance—the two Josephson junctions—so that voltage drops will develop across them. The voltage measured across the junctions is proportional to the magnetic flux over the SQUID's square hole. The feedback coil magnetically couples the SQUID to the pick-up coil in the SQUID sensor. A SQUID is typically 10 to 100 μm on a side. (b) The colored contours show how the magnetic field produced by neural brain currents (dashed arrows) changes in intensity and polarity over the skull's surface. In the red region, the field is most intense in a direction pointing out of the skull. In the blue region, the field is most intense in a direction pointing into the skull.

liquid helium (4 K) contained in a large thermos. The helmet is positioned over a patient's head as he or she sits in a chair (Figure 1).

With sophisticated computer algorithms, MEG data are converted into current maps that give researchers a real-time image of where activity is occurring in the brain. The LANL system responds to brain-current changes in less than a thousandth of a second, adequate for most brain-current studies. The SQUIDs themselves respond in about a millionth of a second. Using specially designed current coils, the LANL MEG system has achieved a spatial resolution of better than 0.25 mm, better than presently reported by any other MEG system (Figure 2).

Eliminating "Noise"

During a MEG measurement, the SQUIDs must be shielded from ambient magnetic fields, whose "noise" tends to swamp the brain signals. Ambient fields are produced mainly by the power lines in a building, although the earth's magnetic field and even the steel in a passing car contribute. (Ferromagnetic materials like steel locally distort the earth's field.) At the frequencies of interest in brain studies—a few to several hundred hertz—the ambient fields must typically be reduced by a factor of 10,000 to 100,000. The helmet's SQUIDs are partially shielded from ambient fields by a thick, hemispherical shell of lead, which becomes superconducting at liquid-helium temperatures. Because superconductors perfectly reflect magnetic fields, the shell reduces ambient fields to as little as one thousandth of their initial strengths. The shielding is not perfect because the shell does not completely enclose the head. The SQUIDs near the shell's crown are better shielded than those near its brim. The shell also reflects the brain's magnetic fields back to the SQUID array, increasing the helmet's sensitivity.

Usually, ambient fields are reduced by taking MEG data in a specially shielded room built with very expensive materials. The superconducting shell effectively blocks magnetic fields from zero to several thousand hertz. Thus, measurements made with the shell require only a "low-end" shielded room, which costs about $100,000—one-fifth that of conventional shielded rooms.

The team has recently added external SQUIDs to the helmet that further reduce the effects of ambient fields. The external SQUIDs measure these fields at several points just outside the superconducting shell, and a computer program then subtracts the fields from the brain-field data to reduce the ambient fields' effects by another factor of 1,000—at all frequencies.

Applications of the MEG/SQUID Technologies

Diagnosing epileptic seizures. For 20% of epilepsy patients, drugs cannot adequately control seizures, and surgically removing the brain tissue where the seizures originate—the epileptigenic tissue—is the only option. But the surgeon must know precisely where the aberrant tissue is to avoid removing nearby tissue required for motor control, sense perception, language, and memory. In addition, by pinpointing how the brain responds to visual, auditory, tactile, or other stimuli, MEG can help

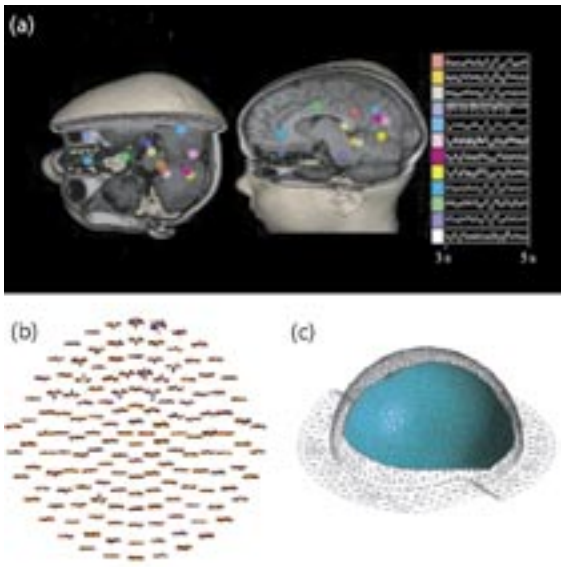

Figure 2. (a) A computer program converts the raw MEG data into maps of the brain's electrical activity as a function of time. These maps can be used to diagnose epilepsy, stroke, and mental disease and to study brain function. (b) The raw data obtained from the 155 SQUID sensors in the MEG helmet. The red waveforms were obtained with the patient's eyes closed. The blue waveforms were obtained as the patient observed a flashing light. (c) The superconducting lead shell. The gray mesh defines the shell's contour. SQUID sensors are attached to the blue surface. At liquid-helium temperatures, the lead shell becomes superconducting and is therefore an excellent magnetic shield. Because a superconductor perfectly reflects magnetic fields at all frequencies, the shell helps shield the underlying SQUID array from ambient magnetic fields. The shell also shields SQUIDs placed outside the shell from the brain's magnetic fields. These external SQUIDs provide data used to help cancel the effects of ambient fields. The superconducting shell and external-field-cancellation method greatly reduce the cost of the magnetically shielded room required for MEG measurements, making them more affordable.

assess the effects of possible collateral damage during surgery.

A brain scan can precisely locate the epileptigenic tissue if the imaging method has high spatial resolution and is fast enough to detect the seizure discharge or the electrical activity that precedes a seizure, which also originates in the epileptigenic tissue. Although seizures occur sporadically, the electrical activity associated with them occurs continually.

Peering into the brain columns. The SQUID team has also developed MicroMEG—using a centimeter-long linear array of SQUIDs with a potential spatial resolution of tens of micrometers. Made of "high-temperature" superconductors, the array's twelve SQUIDs are cooled by liquid nitrogen (77 K) instead of liquid helium (4 K). The MicroMEG array requires less thermal insulation than arrays cooled with liquid helium. Thus, the MicroMEG SQUIDs can be brought within half a millimeter of the tissue under study, allowing extremely high-resolution measurements.

MicroMEG will be used to probe the electrical activity of as few as a few thousand to tens of thousands neurons in one of the brain's cortical columns. The columns are believed to operate in parallel, like the hundreds of microprocessors in a supercomputer that work in parallel to achieve high overall speed. Such studies will improve our understanding of brain function.

Measuring a baby's heartbeat. A variant of MEG called fetal magnetocardiography (FMCG) can be used to diagnose and treat fetal heart conditions. In fact, FMCG is the only way to measure the electrical signals produced by the heartbeat of a baby in the womb. And only the heart's electrical signals contain the detailed timing information required to diagnose and treat fetal arrhythmias. Stethoscopes and ultrasound cannot provide this information because they use sound. Nor is electrocardiography (ECG) useful, because it directly measures the electricity produced by the heart through electrodes taped to the body. However, the baby is electrically insulated from the mother.

Around the twentieth week, the baby's sebaceous glands secrete a waxy, white substance called *vernix caseosa*, which covers the baby's skin to protect it from amniotic fluid in the womb. Because the *vernix* is electrically insulating, electrical signals from the baby's heartbeat cannot pass into the mother's body for measurement on her skin. However, the magnetic fields produced by the baby's heartbeat pass easily through the *vernix* and can be measured with FMCG. Although in principle ECG could be used before the *vernix* forms, the fetal heart is then too small to produce a detectable electrical signal. Unlike other medical diagnostic techniques, FMCG poses no risk to the unborn baby or the mother because it merely receives the magnetic signals sent out by the baby's heart.

References

1. D. Cohen, "Magnetoencephalography: Evidence of magnetic fields produced by alpha-rhythm currents," *Science* **161** 784–786 (1968).
2. D. Cohen, "Magnetoencephalography: Detection of the brain's electrical activity with a superconducting magnetometer," *Science* **175** 664–666 (1970).
3. D. Cohen, E.A. Edelsack, and J.E. Zimmerman, "Magnetocardiograms taken inside a shielded room with a superconducting point contact magnetometer," *Applied Physics Letters* **16** 278–280 (1972).
4. D. Brenner, S.J. Williamson, and L. Kaufman, "Visually evoked magnetic fields of the human brain," *Science* **190** 480–482 (1975).

Acknowledgment

Our work was funded by NIH and the DOE Office of Biological and Environmental Research.

For further information, contact Robert Kraus at 505-665-1938, rkraus@lanl.gov.

Single-Molecule Detection and Characterization

A. Castro, O.C. Marina, F. Martinez (P-21)

Group P-21 efforts in single-molecule detection and spectroscopy focus on the development of novel methods for the ultra-sensitive detection and analysis of biological molecules and their applications to molecular biology and medical diagnosis. Recent developments include the implementation of a technique for the rapid, direct detection of specific nucleic acid sequences in biological samples without the need for enzymatic amplification. Our approach in these experiments is based on detecting the presence of a specific nucleic acid sequence of bacterial, human, plant, or other origin. The nucleic acid sequence may be a DNA or RNA sequence and may be characteristic of a specific taxonomic group, a specific physiological function, or a specific genetic trait. The method we use consists of synthesizing a highly fluorescent nucleic acid reporter molecule using a sequence of the target as a template. A short oligonucleotide primer that is complementary to the target is added to the sample along with a suitable polymerase and free nucleotides. One of these oligonucleotides is partially labeled with a fluorophore. If the target is present in the sample, the primer binds to it, and the polymerase will incorporate the labeled and unlabeled nucleotides, thus reconstructing the target's complementary sequence (Figure 1). The sample is then pumped through the capillary cell of a single-molecule detector. Detection of the reporter signifies the presence of the target being sought. We have applied this method to the detection of specific sequences of DNA from a variety of sources. Most notably, we have demonstrated the detection of DNA from *B. anthracis* at trace concentrations, and in the presence of large amounts of unrelated DNA. *B. anthracis*, the causing agent of anthrax disease, is the weapon of choice in biological warfare. Our recent experiments provide vital research and insight into the intricate workings of specific biological pathogens and supports LANL's defense mission.

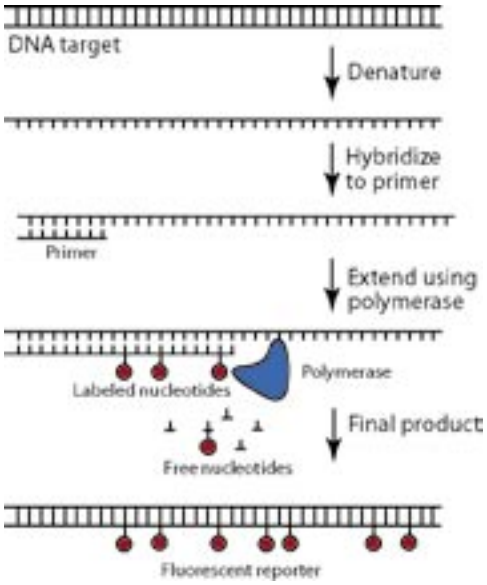

Figure 1. Schematic representation of the polymerase extension reaction for fluorescently labeled reporter molecule synthesis.

Protein Structure, Dynamics, and Function

L.-W. Hung, J. Berendzen, L. Flaks (P-21), T.C. Terwilliger, G.S. Waldo, C.-Y. Kim (B-2), E. Bursey, M. Yu, G. Rajagopalan (Lawrence Berkeley National Laboratory), B. Rupp, B. Segelke (Lawrence Livermore National Laboratory), D. Eisenberg (University of California, Los Angeles), T. Alber (University of California, Berkeley), J. Sacchettini (Texas A&M)

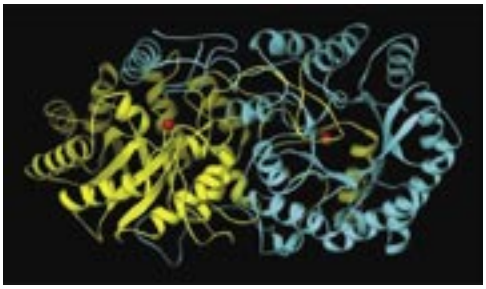

Figure 2. LeuA protein of Mycobacterium tuberculosis (TB), a protein central to Leucine biosynthesis in TB and a potential drug target for TB anti-TB treatment. The structure was determined by Li-Wei Hung (P-21) in collaboration of one of the TBSGC consortium members, Professor Ted Baker of the University of Auckland, New Zealand.

Proteins are the smallest functional unit in living cells. Knowing the structures of proteins is the key to understanding the mechanistic and kinetic modes of these molecular nanomachines. We are pursuing high-throughput x-ray-crystallography technology using high-brilliance synchrotron x-ray beam lines at the Advanced Light Source at Lawrence Berkeley National Laboratory to determine the three-dimensional atomic structures of proteins on a genomic scale. We are one of the integral components of the LANL Tuberculosis Structural Genomics Consortium (TBSGC), one of the ten centers funded by the NIH Protein Structure Initiative to determine a large quantity of novel protein structures in a relatively short amount of time. With the researchers in B Division and LLNL, we established an integrated research resource encompassing the full spectrum of modern structural biology. This includes gene cloning, protein overexpression (B Division), crystallization (LLNL), and x-ray data collection and structure determination (P-21, see Figure 2). Working as a team, we are developing scalable technologies to increase the efficiency and reduce the cost to map each protein structure.

Along with the structural-genomics efforts, we are also developing methods in computational biology to combine protein structure with sequence information to infer their molecular functions. One of the big findings from the completion of genome projects are that over 30%–60% of the genes discovered in most of the organisms have no known functions in humans based on sequence homology alone. These genes and their functions may largely represent the part of biology yet to be discovered. The three-dimensional structures (the shapes) of proteins, have been shown to provide unique information in predicting protein functions. We are working on computational methods to extract structural information to predict protein functions at a much deeper level. From protein sequence and structure to protein function, we are laying out the groundwork to uncover the secret of life.